Journal Pre-proof

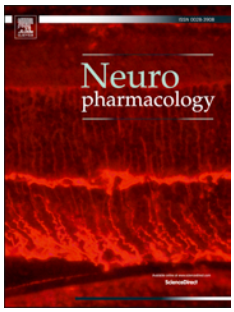

Pre- and postsynaptic modulation of hippocampal inhibitory synaptic transmission by pregnenolone sulphate

Sandra Seljeset, Seth Liebowitz, Damian P. Bright, Trevor G. Smart

PII: S0028-3908(23)00120-X

DOI: https://doi.org/10.1016/j.neuropharm.2023.109530

Reference: NP 109530

To appear in: *Neuropharmacology*

Received Date: 7 November 2022

Revised Date: 28 March 2023

Accepted Date: 31 March 2023

Please cite this article as: Seljeset, S., Liebowitz, S., Bright, D.P., Smart, T.G., Pre- and postsynaptic modulation of hippocampal inhibitory synaptic transmission by pregnenolone sulphate, *Neuropharmacology* (2023), doi: https://doi.org/10.1016/j.neuropharm.2023.109530.

Pre- and postsynaptic modulation of hippocampal inhibitory synaptic transmission by pregnenolone sulphate

By

Author contributions

Sandra Seljeset: Conceptualization, Formal analysis, Methodology, Investigation, Writing - original draft, Writing - review & editing; **Seth Liebowitz**: Investigation; **Damian Bright**: Conceptualization, Formal analysis, Methodology, Investigation, Supervision, Writing - original draft, Writing - review & editing; **Trevor Smart**: Conceptualization, Formal analysis, Methodology, Supervision, Writing - review & editing, Funding acquisition.

Pre- and postsynaptic modulation of hippocampal inhibitory synaptic transmission by pregnenolone sulphate

By

Sandra Seljeset, Seth Liebowitz, Damian P. Bright*

and Trevor G. Smart*

Department of Neuroscience, Physiology & Pharmacology

UCL

Gower Street

London

WC1E 6BT

Correspondence to: Prof T.G. Smart (t.smart@ucl.ac.uk; 0000-0002-9089-5375) and Dr D.P. Bright (d.bright@ucl.ac.uk; 0000-0001-9130-2677)

Abstract

Neurosteroids are important endogenous modulators of $GABA_A$ receptor-mediated neurotransmission within the CNS and play a vital role in maintaining normal healthy brain function. Research has mainly focussed on neurosteroids such as allopregnanolone and tetrahydro-deoxycorticosterone (THDOC) which are allosteric potentiators of $GABA_A$ receptors, whilst the sulphated steroids, including pregnenolone sulphate (PS), which inhibit $GABA_A$ receptor function, have been relatively neglected. Importantly, a full description of PS effects on inhibitory synaptic transmission, at concentrations that are expected to inhibit postsynaptic $GABA_A$ receptors, is lacking. Here, we address this deficit by recording inhibitory postsynaptic currents (IPSCs) from rat hippocampal neurons both in culture and in acute brain slices and explore the impact of PS at micromolar concentrations. We reveal that PS inhibits postsynaptic $GABA_A$ receptors, evident from reductions in IPSC amplitude and decay time. Concurrently, PS also causes an increase in synaptic GABA release which we discover is due to the activation of presynaptic TRPM3 receptors located close to presynaptic GABA release sites. Pharmacological blockade of TRPM3 receptors uncovers a PS-evoked reduction in IPSC frequency. This second presynaptic effect is caused by PS activation of inwardly-rectifying Kir2.3 channels on interneurons, which act to depress synaptic GABA release. Overall, we provide a comprehensive characterisation of pre- and postsynaptic modulation by PS of inhibitory synaptic transmission onto hippocampal neurons which elucidates the diverse mechanisms by which this understudied neurosteroid can modulate brain function.

Pre- and postsynaptic modulation of hippocampal inhibitory synaptic transmission by pregnenolone sulphate

By

Sandra Seljeset, Seth Liebowitz, Damian P. Bright*

and Trevor G. Smart*

Department of Neuroscience, Physiology & Pharmacology

UCL

Gower Street

London

WC1E 6BT

Correspondence to: Prof T.G. Smart (t.smart@ucl.ac.uk; 0000-0002-9089-5375) and Dr D.P. Bright (d.bright@ucl.ac.uk; 0000-0001-9130-2677)

Highlights

- Pregnenolone sulphate (PS) is an endogenous brain neurosteroid
- PS modulates hippocampal inhibitory synaptic transmission
- PS blocks postsynaptic $GABA_A$ receptors to decrease IPSC amplitude and decay time
- PS activates presynaptic TRPM3 channels to increase synaptic GABA release
- Block of TRPM3 reveals a PS-evoked reduction in GABA release via Kir2 channels

Abstract

Neurosteroids are important endogenous modulators of $GABA_A$ receptor-mediated neurotransmission within the CNS and play a vital role in maintaining normal healthy brain function. Research has mainly focussed on neurosteroids such as allopregnanolone and tetrahydro-deoxycorticosterone (THDOC) which are allosteric potentiators of $GABA_A$ receptors, whilst the sulphated steroids, including pregnenolone sulphate (PS), which inhibit $GABA_A$ receptor function, have been relatively neglected. Importantly, a full description of PS effects on inhibitory synaptic transmission, at concentrations that are expected to inhibit postsynaptic $GABA_A$ receptors, is lacking. Here, we address this deficit by recording inhibitory postsynaptic currents (IPSCs) from rat hippocampal neurons both in culture and in acute brain slices and explore the impact of PS at micromolar concentrations. We reveal that PS inhibits postsynaptic $GABA_A$ receptors, evident from reductions in IPSC amplitude and decay time. Concurrently, PS also causes an increase in synaptic GABA release which we discover is due to the activation of presynaptic TRPM3 receptors located close to presynaptic GABA release sites. Pharmacological blockade of TRPM3 receptors uncovers a PS-evoked reduction in IPSC frequency. This second presynaptic effect is caused by PS activation of inwardly-rectifying Kir2.3 channels on interneurons, which act to depress synaptic GABA release. Overall, we provide a comprehensive characterisation of pre- and postsynaptic modulation by PS of inhibitory synaptic transmission onto hippocampal neurons which elucidates the diverse mechanisms by which this understudied neurosteroid can modulate brain function.

Keywords

$GABA_A$ receptors, pregnenolone sulphate, synaptic inhibition, TRPM3 receptors, Kir2.3 channels, GABA release.

Introduction

The $GABA_A$ receptor is the principal mediator of fast inhibitory neurotransmission in the central nervous system (Smart & Paoletti, 2012). To enable normal, healthy brain function, $GABA_A$-mediated inhibition is regulated and fine-tuned by an array of mechanisms, including direct modulation of $GABA_A$ receptors by endogenous ligands, the most extensively studied of which are the neurosteroids (Belelli & Lambert, 2005). Prior studies have largely focussed on the 3α-hydroxy-pregnane neurosteroids, which include allopregnanolone and tetrahydro-deoxycorticosterone (THDOC). These mediate their actions primarily via potentiating the activation of $GABA_A$ receptors by GABA by binding directly to the receptor at allosteric sites (Laverty *et al.*, 2017; Miller *et al.*, 2017). However, another important but less well-studied class of these endogenous modulators, are the sulphated neurosteroids, including pregnenolone sulphate (PS) and dehydroepiandrosterone sulphate, which inhibit $GABA_A$ receptors (Belelli & Lambert, 2005; Seljeset *et al.*, 2015). These latter modulators are thought to play key roles in memory and cognition (Mayo *et al.*, 1993; Flood *et al.*, 1999; Smith *et al.*, 2014). Their significance for maintaining normal brain function is emphasised by observations that dysregulated sulphated neurosteroid levels are associated with Alzheimer's disease, schizophrenia, anxiety disorders and depression (Weill-Engerer *et al.*, 2002; Maninger *et al.*, 2009; Wong *et al.*, 2015; Vankova *et al.*, 2016). These steroid molecules are capable of modulating various ion channels and receptors that may be important for mediating their actions on neural function, including specific voltage-gated sodium, calcium and potassium channels, the transient receptor potential cation channel family M member 3 (TRPM3), sigma-1 receptor (σ1), AMPA/Kainate, NMDA and $GABA_A$ receptors (Smith *et al.*, 2014). However, the higher potency of sulphated neurosteroids, particularly PS, at $GABA_A$ receptors, combined with the ubiquitous physiological significance of these receptors for neurotransmission and brain function, suggests that these receptors are important CNS targets.

Modulation of the $GABA_A$ receptor by PS has been extensively studied and characterised in recombinant expression systems (Akk *et al.*, 2001, 2007; Eisenman *et al.*, 2003; Seljeset *et al.*, 2015, 2018). However, the role of PS in regulating synaptic GABAergic neurotransmission has been less well described (Teschemacher *et al.*, 1997; Mtchedlishvili & Kapur, 2003). The few studies to have

been performed have highlighted the divergent presynaptic actions of PS in decreasing and increasing respectively, synaptic GABA release onto cultured hippocampal neurons (Teschemacher *et al.*, 1997; Mtchedlishvili & Kapur, 2003) and cerebellar Purkinje cells (Zamudio-Bulcock & Valenzuela, 2011). Nevertheless, evidence for direct modulation of $GABA_A$ receptors during synaptic neurotransmission is however scarce, with only one of these studies showing an effect (a reduction in IPSC amplitude) consistent with PS inhibition of postsynaptic $GABA_A$ receptors (Zamudio-Bulcock & Valenzuela, 2011). Notably, none of these studies have examined modulation of the decay phase of inhibitory postsynaptic currents (IPSCs) within the low micromolar range of PS concentrations known to inhibit recombinant $GABA_A$ receptors (Seljeset *et al.*, 2018).

To explore thoroughly how PS modulates inhibitory synaptic transmission, we have investigated the impact of micromolar concentrations of this neurosteroid on IPSCs recorded from hippocampal neurons both in culture and in acute brain slices. We report that PS decreases both IPSC amplitude and decay time, consistent with an inhibitory effect on postsynaptic $GABA_A$ receptors. Concurrent with its postsynaptic impact, PS also acts upon populations of presynaptic TRPM3 and potassium channels to increase and decrease synaptic GABA release respectively, with the former effect being predominant. These results therefore help us to further understand the complexity of pre- and postsynaptic mechanisms by which this understudied endogenous compound modulates inhibitory synaptic transmission within the brain.

Methods

Ethical approval

All procedures involving animals complied with the ARRIVE guidelines (ARRIVE guidelines | NC3Rs) and were performed in accordance with UK Home Office regulations under the *Animals (Scientific Procedures) Act, 1986.* Sprague-Dawley rats were maintained under a standard 12:12 hour light/dark cycle and were allowed *ad libitum* access to food and water.

Hippocampal cell culture

Hippocampal cultures were prepared from E18 Sprague-Dawley rat embryos. Dissected hippocampi were incubated at 37 °C in trypsin solution (0.1% w/v in Hank's balanced salt solution (HBSS); Gibco) for 10 min, before four washes in HBSS. Neurons were dissociated by mechanical trituration using fire-polished glass Pasteur pipettes in plating medium (minimum essential medium (MEM) supplemented with 2 mM L-glutamine, 10 U/mL penicillin-G, 10 µg/mL streptomycin, 20 mM glucose, 5% v/v horse serum and 5% v/v heat-inactivated foetal calf serum (all from Gibco)). The cell suspension was centrifuged for 10 min at 168 x *g*, before resuspension in fresh plating medium and seeding onto poly-L-ornithine-coated coverslips. The cells were left for at least one hour at 37 °C in humidified air with 5% CO_2 before the plating medium was replaced with a maintenance medium containing: Neurobasal-A supplemented with 0.5% GlutaMAX, 50 U/mL penicillin-G, 50 µg/mL streptomycin, 1% v/v B-27 supplement and 35 mM glucose (all from Gibco).

Acute brain slice preparation

Young rats (P14) were anaesthetised with isoflurane and decapitated, before rapid removal of the brain. Coronal sections of the hippocampus (250 µm) were prepared using a Leica VT 1200s vibroslicer with the brain immersed in ice-cold slicing solution composed of (mM): 130 K-gluconate, 15 KCl, 0.05 EGTA, 20 HEPES, 4 Na-pyruvate, 25 glucose and 2 kynurenic acid (pH 7.4). Brain slices were subsequently transferred to a holding chamber incubated at 37 ºC where the slicing solution was slowly exchanged (over ~ 1 hour) for artificial cerebrospinal fluid (aCSF) containing (mM): 125 NaCl, 2.5 KCl, 1.25 NaH_2PO_4, 26 $NaHCO_3$, 2 $CaCl_2$, 1 $MgCl_2$, 25 glucose

and 2 kynurenic acid (pH 7.4 when bubbled with 95 % O_2 and 5 % CO_2). Slices were maintained in the holding chamber at room temperature until required for electrophysiology.

Recording from hippocampal neurons in culture and in slices

Whole-cell recordings were made from cultured hippocampal neurons (DIV 10-16) continuously superfused with room temperature Krebs solution containing (in mM): 140 NaCl, 4.7 KCl, 1.2 $MgCl_2$, 2.52 $CaCl_2$, 11 glucose and 5 HEPES, adjusted to pH 7.4 with 1 M NaOH, supplemented with 1 mM kynurenic acid (Sigma) to block excitatory glutamatergic transmission. Brain slices were superfused with room temperature aCSF and whole-cell recordings made from hippocampal CA1 pyramidal neurons visualised using infra-red differential interference contrast (IR-DIC) optics. Patch pipettes had resistances of 2.5 - 4 MΩ and were filled with an internal solution containing (in mM): 140 CsCl, 2 NaCl, 10 HEPES, 5 EGTA, 2 $MgCl_2$, 0.5 $CaCl_2$, 2 NaATP and 0.5 NaGTP (pH 7.3, osmolarity 300 ± 10 mOsm).

Membrane currents were recorded from hippocampal neurons voltage-clamped at -60 mV using either an Axopatch 200B or Multiclamp 700B amplifier (both Molecular Devices). Currents were filtered at 2 kHz, digitised at 20 kHz via either a Digidata 1440A (Molecular Devices) or Power 1401 (Cambridge Electronic Design) interface and acquired using Clampex 10.3 (Molecular Devices) or WinEDR (Version 3.5.2, John Dempster, Strathclyde University) software. Series resistance was monitored throughout all recordings by measuring the membrane current responses to 10 mV hyperpolarising voltage steps. If the series resistance varied by more than 30%, cells were discarded. All solutions were bath applied.

Analysis of neuronal recordings

For the analysis of GABA-mediated inhibitory postsynaptic currents (IPSCs), event detection was performed using WinEDR software (Version 3.5.2) by using an amplitude-threshold crossing method. All detected events were manually checked before further analysis was carried out in WinWCP (Version 4.8.6, John Dempster) to calculate event amplitudes and the frequency of IPSCs under different recording conditions. All validated IPSCs were included for the analyses of event amplitude and frequency, whilst only “clean” events that showed monotonic rises and uncontaminated decay phases were used for kinetic analysis (> 50 events in each

condition). These were aligned on their rising phases and averaged to produce mean IPSC waveforms. Weighted tau decay (τ_w) values were calculated by fitting a biexponential curve to the decay phase of the mean IPSC waveform and applying the equation:

$$\tau_w = \frac{A_1.\tau_1 + A_2.\tau_2}{A_1 + A_2},$$

where τ_1 and τ_2 represent time constants for the two exponential components of the decay phase, and A_1 and A_2 are their relative amplitude contributions.

To analyse changes in spontaneous IPSC (sIPSC) amplitudes, distributions of sIPSC amplitudes were generated before and during drug application. The sIPSC amplitude distributions were fitted using a sum of Gaussians based on the function described below:

$$y = y_0 + \sum_{i=1}^{n} Ae^{\frac{-(X-Xc)^2}{2w^2}},$$

where each Gaussian is defined by parameters for amplitude, A*,* mean, *Xc* and variance, *w*, and where y_0 represents the baseline amplitude of the distribution. Fits were determined using a non-linear least squares Marquardt routine within Origin (Microcal ver 6) software.

For the amplitude distributions of sIPSCs, equal numbers (200 per cell) of sIPSCs were sampled in each condition. In PS, sIPSCs were sampled 2 min after the onset of drug application to ensure the effect of the neurosteroid had reached equilibrium.

Immunocytochemistry and imaging

Immunocytochemistry was performed in cultured hippocampal neurons (DIV 14) using the following primary antibodies: rabbit anti-TRPM3 (ACC-050, Alomone, 1:200), rabbit anti-Kir2.3 (APC-032, Alomone, 1:200), mouse anti-GAD65 (ab85866, Abcam, 1:200), mouse anti-gephyrin (#147 111, Synaptic Systems, 1:200) and mouse anti-MAP2 (GTX11267, GeneTex, 1:500). Neurons were briefly washed with PBS, before fixation in PFA (4% v/v paraformaldehyde/ 4% w/v sucrose in PBS, pH 7.2). After further washing to remove PFA, neurons were permeabilised with a block solution (10 % v/v goat serum, 1 % w/v BSA in PBS) containing 0.1% v/v Triton X-100 for 5 min and then incubated with block solution for a further 20 min at room

temperature. Intracellular antigens were then labelled by primary antibody incubation for 1 hour at room temperature. For negative control experiments, the TRPM3 and Kir2.3 antibodies were preincubated with negative control peptides (50 µg/ml) for 1 hour at room temperature. Neurons were then washed and incubated with appropriate Alexa Fluor-conjugated secondary antibodies for 1 hour (ThermoFisher Scientific, 1:1000). After extensive washing, coverslips were mounted on slides with Prolong Glass mounting medium (ThermoFisher Scientific). Subsequent imaging was performed using a Zeiss LSM-510 confocal microscope equipped with a 40X oil objective (1.4 NA). Images were digitally captured using Zeiss LSM software.

Statistics

For all datasets, the Kolmogorov-Smirnov test was used to check for normality. In nearly all cases, data were distributed normally, with the exception being the datasets describing PS effects on mIPSC frequency (Fig. 3A, B) and PS and ononetin effects on sIPSC frequency (Fig. 4A, B). In these cases, logarithmic transformation was found to produce normally distributed values and therefore, further parametric comparisons were performed on the transformed datasets. Pairwise comparisons were made using a paired two-tailed t-test. For many of the experiments, effects of different concentrations of PS were compared with their own paired control recordings – statistical comparison for these experiments was undertaken using two-way repeated measures (RM) ANOVA, followed by Sidak's multiple comparison tests. For cases involving more than two groups, comparison was accomplished using one-way RM ANOVA, followed by Tukey's multiple comparison tests. All statistical analyses were carried out using GraphPad Prism (version 9.3.1, GraphPad Software), with the threshold for statistical significance set at $p < 0.05$. Data are reported as mean ± SEM throughout with n numbers indicating numbers of cells. Values for mean sIPSC and mIPSC frequencies and amplitudes for all experiments are presented in Table 1.

Results

PS increases sIPSC frequency in hippocampal neurons

To investigate the impact of PS on inhibitory synaptic transmission, spontaneous inhibitory postsynaptic currents (sIPSCs) were recorded from hippocampal pyramidal neurons in culture (DIV 10-16). Application of PS (30 nM - 10 μM) caused a concentration-dependent modulation of synaptic GABA release, with a large increase in sIPSC frequency evident at higher PS concentrations (drug effect $F(1,31) = 20.06$, $p < 0.0001$, two-way RM ANOVA; Fig. 1A, B; Table 1). Compared to control, the fold increase in sIPSC frequency was 1.8 ± 1.0 at 30 nM PS ($p = 0.997$, $n = 6$), 2.5 ± 1.1 at 1 μM ($p = 0.697$, $n = 6$), 6.6 ± 2.0 at 3 μM ($p = 0.009$, $n = 11$) and 9.5 ± 3.6 at 10 μM PS ($p < 0.0001$, $n = 12$, all by Sidak's multiple comparisons tests after two-way RM ANOVA). The increase in sIPSC frequency was relatively fast, appearing to saturate within 2 min of exposure to PS, was relatively well-sustained over 5 min in PS and was reversible upon washout of PS (Fig. 1C).

PS inhibits postsynaptic $GABA_A$ receptors

In parallel with its presynaptic effect on sIPSC frequency, PS also modulated sIPSC amplitude and decay. Mean sIPSC waveforms show that PS causes an inhibition of the peak amplitude and accelerates the sIPSC decay phase (Fig. 2A; Table 1). Examination of the PS concentration-dependence of the effect on sIPSC amplitude reveals that whilst there is no significant impact at a low concentration (30 nM), higher concentrations inhibit sIPSC amplitude to a similar degree (drug effect $F(1,31) = 28.97$, $p < 0.0001$, two-way RM ANOVA; Fig. 2B). The mean sIPSC amplitude was 90.9 ± 13.2% of control ($p = 0.747$, $n = 6$) at 30 nM PS compared to 62.0 ± 14.2% ($p = 0.0011$, $n = 6$), 68.9 ± 8.0% ($p = 0.0277$, $n = 11$) and 68.0 ± 8.4% ($p = 0.0241$, $n = 12$, all by Sidak's multiple comparisons tests after two-way RM ANOVA) at 1 μM, 3 μM and 10 μM, respectively. Analysis of the effect of 10 μM PS on sIPSC decay times was precluded by the large increase in sIPSC frequency at this concentration and the resulting difficulty in finding "clean" sIPSCs. However, at lower concentrations, PS caused a concentration-dependent acceleration of the sIPSC decay with normalised decay times of 83.7 ± 2.6% ($p = 0.0085$, $n = 5$) and 62.5 ± 2.6% ($p < 0.0001$, $n = 8$, both by Sidak's multiple comparisons tests after two-way

RM ANOVA, drug effect $F(1,10) = 100.4$, $p < 0.0001$) relative to control in the presence of 1 µM and 3 µM PS respectively (Fig. 2C).

To further investigate the effect of PS on the size of synaptic currents, sIPSC amplitude distributions were generated and fitted with the sum of multiple Gaussians (Fig. 2D-G). In neurons treated with 3 µM PS, the distribution of IPSC amplitudes was similar to control, with the populations of events in both conditions being best described by the sum of two Gaussians (Fig 2D, E). In control, the two Gaussians had means (± standard deviation) of 26.9 ± 0.2 pA and 54.3 ± 3.1 pA, whilst in 3 µM PS the means were 24.3 ± 0.5 pA and 52.6 ± 7.2 pA. This suggests that there is little effect of 3 µM PS on the sIPSC peak amplitude, and that the reduction in the mean sIPSC amplitude reflects an increased frequency of small events (< 30 pA) compared with control.

When neurons were treated with 10 µM PS, only one population of sIPSC amplitudes was evident as the data were best described by a single Gaussian fit with a mean of 29.5 ± 0.4 pA, whereas the two populations in control had means of 30.0 ± 0.2 pA and 62.6 ± 5.0 pA (Fig. 2F,G). This analysis shows that the population of larger sIPSCs (> 50 pA) is absent in 10 µM PS. The reduced frequency of large amplitude sIPSCs may reflect possible multivesicular release of GABA (Auger *et al.*, 1998; Barberis *et al.*, 2004) causing synaptic receptors to adopt a desensitised state that is more prone to block by PS (Seljeset *et al.*, 2018). We propose that this is not a significant factor for the low amplitude sIPSCs that are probably more reliant on single vesicular release. Overall, the decreased sIPSC amplitude and decay time in PS are consistent with a direct inhibition of postsynaptic $GABA_A$ receptors, concurrent with the presynaptic impact of PS increasing GABA release.

PS has pre- and postsynaptic effects on mIPSCs

Various ion channels and receptors are potential presynaptic targets of PS. To increase GABA release, PS could act by increasing the excitability of presynaptic interneurons, or more locally, to increase Ca^{2+} concentration in the synaptic terminal. Alternatively, it might also interact directly with the synaptic release machinery to increase the probability of vesicular GABA release.

To assess whether PS increases presynaptic GABA release by increasing the excitability of presynaptic neurons, recordings were made in the presence of TTX

(500 nM) to block action potentials (APs) and the effects of PS (1-10 µM) on AP-independent mIPSCs were investigated. Similar to the results obtained in the absence of TTX, PS evoked a concentration-dependent increase in mIPSC frequency (drug effect $F(1,19) = 71.93$, $p < 0.0001$, two-way RM ANOVA on logarithmic transforms of the datasets; Fig. 3A, B). At 1 µM PS, the frequency did not increase significantly (1.1 ± 0.1-fold compared with control, $p > 0.9999$, $n = 8$), but at 3 µM, the fold-increase in frequency relative to control was 3.0 ± 0.6 ($n = 0.0034$, $n = 8$), and at 10 µM PS, there was a striking 20.6 ± 5.3-fold increase in mIPSC frequency ($p < 0.0001$, $n = 6$, all by Sidak's multiple comparisons tests after two-way RM ANOVA). These results indicate that the increase in GABA release is not due to PS stimulating AP firing in presynaptic interneurons.

In contrast to sIPSCs, PS did not reduce mIPSC peak amplitudes (drug effect $F(1,19) = 2.752$, $p = 0.1136$, two-way RM ANOVA). At 1 µM PS the mIPSC peak amplitude was 94.9 ± 4.7% of control ($p = 0.9391$, $n = 8$), at 3 µM it was 89.4 ± 6.2% ($p = 0.4051$, $n = 8$) of control, and at 10 µM PS, the peak amplitude was 97.8 ± 12.4% of control ($p = 0.7612$, $n = 6$, all by Sidak's multiple comparisons tests after two-way RM ANOVA; Fig. 3C; Table 1). The lack of impact of PS on the size of mIPSCs was confirmed by plotting amplitude distributions and fitting with the sum of multiple of Gaussians (Fig. 3F,G & H). For all three concentrations of PS tested, mIPSC amplitude distributions were best-fit by the sum of two Gaussians and these Gaussians did not shift when comparing events in PS to those recorded in control (Gaussian means ± SDs: 1 µM PS 25.8 ± 0.2 pA and 43.1 ± 2.2 pA compared with control 24.6 ± 0.4 pA and 42.3 ± 4.3 pA; 3 µM PS 25.6 ± 0.2 pA and 44.0 ± 3.4 pA compared with control 24.6 ± 0.5 pA and 41.8 ± 3.4 pA; 10 µM PS 25.1 ± 0.8 pA and 43.2 ± 7.5 pA compared with control 22.3 ± 1.2 pA and 37.1 ± 12.4 pA).

To determine if PS also increased the rate of mIPSC decay, mean mIPSC waveforms in control and in the presence of PS (1-10 µM) were constructed and weighted decay time constants (τ_w) determined (Fig. 3D, E). PS had a concentration-dependent effect on the mIPSC decay time with τ_w reduced to 96.2 ± 10.1% ($p = 0.8781$, $n = 8$), 76.6 ± 2.2% ($p = 0.0423$, $n = 8$) and 49.5 ± 7.9% ($p < 0.0001$, $n = 6$, all by Sidak's multiple comparisons tests after two-way RM ANOVA, drug effect $F(1,19) = 32.75$, $p < 0.0001$) of control in the presence of 1 µM, 3 µM or 10 µM PS, respectively. TTX itself did not have any effect on IPSC decay - comparing τ_w in cells

with and without 500 nM TTX, showed that τ_w is 33.2 ± 6.1 ms in control and 34.6 ± 8.7 ms in TTX ($t(24) = 0.4826$, $p = 0.6337$, $n = 13$, two sample equal variance t-test, two-tailed; data not shown). Taken together, the data for mIPSCs show that, in the absence of action potentials, PS still acts on a presynaptic target to increase synaptic GABA release, whilst concurrently modulating postsynaptic $GABA_A$Rs to curtail IPSC duration.

PS increases synaptic GABA release via TRPM3 channels

The TRPM3 receptor is a well-documented target of PS (Wagner *et al.*, 2008; Vriens *et al.*, 2011), and is widely expressed in the human and rodent brain (Lee *et al.*, 2003; Fonfria *et al.*, 2006; Kunert-Keil *et al.*, 2006; Zamudio-Bulcock & Valenzuela, 2011; Held *et al.*, 2015). PS acts as an agonist at the TRPM3 receptor, increasing the flux of cations through the intrinsic ion channel. The TRPM3 channel permeability for Ca^{2+} is 10 times that for monovalent cations (Held *et al.*, 2015), and could therefore promote neurotransmitter release. To investigate if TRPM3 could be the presynaptic target of PS involved in increasing synaptic GABA release, we used the TRPM3-selective antagonist ononetin at 10 µM, a concentration that should produce a complete block of the TRPM3 receptor (Straub *et al.*, 2013). At this concentration, ononetin was found to have no activity at recombinant $GABA_A$ receptors expressed in HEK cells (data not shown).

Ononetin alone did not affect the frequency of sIPSCs (92.3 ± 19.0% of control; $p = 0.4204$, Tukey's multiple comparisons test after one-way RM ANOVA on logarithmic transforms of the data, $n = 11$; Fig. 4 A, B; Table 1) suggesting no constitutive TRPM3 activity. When PS (10 µM) was co-applied in the presence of ononetin, instead of an increase in sIPSC frequency, IPSCs occurred significantly less frequently compared to ononetin alone (43.7 ± 9.0%, $p = 0.0022$, Tukey's multiple comparisons test after one-way RM ANOVA, $F(2,20) = 14.87$, $p = 0.0001$; Fig. 4 A, B). These results suggest that blocking TRPM3 prevents the PS-induced increase in GABA release, and that PS also acts at an additional presynaptic target to reduce GABA release, an effect that is only revealed when TRPM3 is blocked.

Examination of sIPSC amplitudes showed that ononetin had no effect on the mean sIPSC peak amplitude (110.0 ± 16.3% normalised to control, $p = 0.9988$, Tukey's multiple comparisons test after one-way RM ANOVA, $n = 10$; Fig. 4C). However,

when PS was co-applied, there was a significant reduction in the size of sIPSCs (66.0 ± 7.4% normalised to control, p = 0.0089 compared to ononetin alone, Tukey's multiple comparisons test after one-way RM ANOVA, F(2,18) = 7.502, p = 0.0043; Fig. 4C).

Further confirmation of the role of presynaptic TRPM3 channels was established by investigation of the effect of PS on mIPSCs recorded in the presence of ononetin (10 µM; Fig. 4D, E & F). As with sIPSCs, application of PS (10 µM) during TRPM3 blockade, caused a significant decrease in mIPSC frequency (64.7 ± 11.5% normalised to ononetin alone, p = 0.032, paired t test, t = 2.281, n = 7; Fig. 4E). Also consistent with our recordings of sIPSCs, PS application in the presence of ononetin caused a reduction in mIPSC amplitude (68.0± 3.5% normalised to ononetin alone, p = 0.012, paired t test, t = 5.044, n = 7; Fig. 4F). Hence, blockade of TRPM3 prevents the PS-evoked increase in GABA release apparent as frequency increases in both sIPSCs and mIPSCs under control conditions and reveals an additional presynaptic target that instead mediates a PS-dependent decrease in GABA release.

The neuronal recordings indicate that PS activates presynaptic TRPM3 channels located on interneurons to increase synaptic GABA release. Furthermore, the observation that PS is still able to increase GABA release in the presence of TTX suggests that these TRPM3 channels are likely to be located either at, or close to presynaptic GABA release sites. To investigate the expression and localisation of TRPM3 channels in our cultured neurons, immunocytochemistry was performed using an anti-TRPM3 antibody. Initially, specificity of this antibody was confirmed by pre-adsorption with a negative control peptide, which blocked neuronal labelling as expected (Fig. 4G). In the absence of the negative control peptide, TRPM3 immunoreactivity showed a punctate distribution along MAP2-positive neuronal dendrites (Fig. 4G). Further immunostaining was performed using co-labelling with antibodies directed against two different inhibitory synaptic markers, either the GABA-synthetic enzyme, GAD65 (presynaptic, Fig. 4H) or the inhibitory synapse scaffolding protein, gephyrin (postsynaptic, Fig. 4I). TRPM3 immunoreactivity showed some degree of colocalization with both inhibitory synaptic markers, indicating that this channel is likely to be expressed at a subset of inhibitory synapses corroborating its role in mediating the PS-evoked increase in synaptic GABA release.

PS decreases synaptic GABA release via Kir2.3 channels

Application of PS when TRPM3 channels are blocked with ononetin causes a significant reduction in both sIPSC and mIPSC frequency (Fig. 4A, B, D & E), suggesting the presence of an additional presynaptic PS target that causes a depression in synaptic GABA release. One potential candidate is inward-rectifier K^+ channels, since these, in particular the homomeric Kir2.3 channel and Kir2.3-containing heteromeric channels, are sensitive to potentiation by PS (Kobayashi *et al.*, 2009). Activation of the Kir2.3 channel has previously been shown to produce membrane hyperpolarisation (Liu *et al.*, 2002) – hence, PS could lead to hyperpolarisation of presynaptic terminals and a reduction in synaptic release.

Ba^{2+} is an effective blocker of Kir channels (Dascal *et al.*, 1993; Tanemoto *et al.*, 2002; Kobayashi *et al.*, 2009), and produces a full block of Kir2.3 currents at 3 mM (Kobayashi *et al.*, 2009). To determine if PS reduces synaptic GABA release by activating Kir channels, PS was applied in the presence of 3 mM Ba^{2+} and 10 µM ononetin.

Neurons were first exposed to 3 mM Ba^{2+} to determine the effect of this blocker on baseline activity, before co-application of 10 µM ononetin and 10 µM PS. Applying Ba^{2+} alone produced a large increase in the frequency of sIPSCs compared to baseline activity (14.3 ± 3.7-fold; $p = 0.0064$, Tukey's multiple comparisons test after one-way RM ANOVA, $n = 7$; Fig. 5 A, B; Table 1). Interestingly, the sIPSC frequency did not change greatly upon further co-application of ononetin and PS, the fold increase compared to control being 20.8 ± 6.3 ($p = 0.5738$, Tukey's multiple comparisons test after one-way RM ANOVA, $F(3,15) = 10.99$, $p = 0.0005$). This finding supports a role for Kir channels in mediating the PS-induced decrease in GABA release.

IPSCs were smaller in Ba^{2+} with amplitudes decreased to 62.2 ± 8.3% of control ($p = 0.003$, Tukey's multiple comparisons test after one-way RM ANOVA, $n = 7$). When PS and ononetin were applied, IPSC amplitudes were further reduced to 33.5 ± 4.7% of control, signifying a trend towards even smaller amplitudes than in Ba^{2+} alone ($p = 0.068$, Tukey's multiple comparisons test after one-way RM ANOVA, $F(3,15) = 18.74$, $p < 0.0001$).

Whilst providing support for the idea that PS might act via inward rectifier K^+ channels, Ba^{2+} lacks selectivity and also blocks other types of K^+ channels. Therefore, we used ML133, a selective blocker of Kir2 channels, including Kir2.1, Kir2.2, Kir2.3 and Kir2.6 (Wu *et al.*, 2010; Wang *et al.*, 2011). To corroborate the results obtained using Ba^{2+}, neurons were kept in 10 µM ononetin throughout the experiment, with sequential co-application of ML133 (100 µM) and PS (10 µM).

Co-application of ML133 produced a large increase in the frequency of sIPSCs (12.7 ± 1.8-fold) relative to ononetin alone ($p = 0.0001$, Tukey's multiple comparisons test after one-way RM ANOVA, n = 8; Fig. 5 C, D; Table 1). When PS was subsequently applied in the presence of both ononetin and ML133, there was no effect on sIPSC frequency ($p = 0.8378$ compared to ononetin and ML133, with a fold increase relative to the ononetin control of 11.9 ± 1.9, $p = 0.0003$, Tukey's multiple comparisons tests after one-way RM ANOVA, $F(2,14) = 20.84$, $p < 0.0001$). Therefore, these results suggest that PS acts to decrease GABA release from the presynaptic terminal by potentiating Kir2 channels, most likely either Kir2.3 homomeric or heteromeric channels. This effect is only apparent when the potentiating effect of PS on synaptic GABA release is prevented by blocking the TRPM3 receptor.

The mean sIPSC amplitude in the presence of ML133 was 80.8 ± 13.6% compared to the ononetin control ($p = 0.1031$, Tukey's multiple comparisons test after one-way RM ANOVA, n = 8). Compared to the ononentin control, the mean sIPSC amplitude in the presence of PS, ML133 and ononetin was 67.6 ± 11.6% ($p = 0.8561$, Tukey's multiple comparisons test after one-way RM ANOVA, $F(2,14) = 4.251$, $p = 0.0361$).

To confirm the expression of Kir2.3-containing K channels in the cultured neurons, we performed immunocytochemistry using an anti-Kir2.3 antibody. Specificity of this antibody was demonstrated by using pre-adsorption with a negative control peptide. Kir2.3 immunostaining showed a clustered distribution along MAP2-positive neuronal dendrites that was eliminated by pre-adsorption with the control peptide (Fig. 5G). Co-labelling with GAD65 and gephyrin demonstrated that Kir2.3 shows partial colocalization with both of these inhibitory synaptic markers, indicating expression at a subset of GABAergic synapses (Fig. 5E,F). This supports the functional data in indicating that PS causes a decrease in synaptic GABA release by positive modulation of presynaptic Kir2.3-containing inward rectifier K^+ channels.

PS increases synaptic GABA release onto CA1 PCs via TRPM3 channels

Our recordings from cultured hippocampal neurons reveal that application of PS evokes both pre- and postsynaptic effects on inhibitory synaptic transmission. As expected from studies using recombinant receptors, PS blocks postsynaptic $GABA_A$Rs, resulting in reductions in IPSC amplitude and decay time. Unexpectedly, PS also causes a striking increase in IPSC frequency. This presynaptic effect on GABA release is mediated by PS activating presynaptic TRPM3 channels located at, or close to inhibitory terminals on interneurons. To assess whether this same mechanism occurs under more physiological conditions, we recorded from CA1 pyramidal cells (PCs) in acute brain slices.

Application of PS (10 µM) evoked an increase in synaptic GABA release onto CA1 PCs (Fig. 6A, B). The increase in sIPSC frequency was less than that observed in our cultured hippocampal neurons but was still significant (299.1 ± 79.1%, p = 0.012, paired t test, t = 3.854, n = 6; Fig. 6B; Table 1). Whilst there was no effect on sIPSC amplitude (mean amplitude in PS of 97.9 ± 5.8% normalised to control, p = 0.46, paired t test, t = 0.8001, n = 6), a postsynaptic modulation of $GABA_A$Rs by PS was revealed by a reduction in sIPSC decay time (71.6 ± 6.8% normalised to control, p = 0.006, paired t test, t = 3.873, n = 6; Fig. 6B). To ascertain whether the increase in GABA release is driven by PS activation of TRPM3 channels, we used the selective blocker ononetin. Application of ononetin (10 µM) alone, caused a significant increase in sIPSC frequency (212.9 ± 42.1% normalised to control, p = 0.03, Tukey's multiple comparisons test after one-way RM ANOVA, n = 6; Fig. 6C, D). The mechanism causing this unexpected increase in sIPSC frequency is unclear but may reflect a more complex disinhibition between interneurons than we observe in our cultured neurons. However, upon co-application of PS in the presence of ononetin, there was no further increase in sIPSC frequency (253.4 ± 45.6% normalised to control, p = 0.65 compared with ononetin alone, Tukey's multiple comparisons test after one-way RM ANOVA, F(2,10) = 8.242, p = 0.0077; Fig. 6C, D). Hence, PS also causes an increase in synaptic GABA release onto CA1 PCs in acute brain slices via activation of presynaptic TRPM3 channels.

Discussion

Neurosteroids synthesised within the brain play a vital role in maintaining normal healthy brain function, mainly through modulating inhibitory transmission mediated by $GABA_A$ receptors. These neurosteroids are capable either of potentiating $GABA_A$ receptors to promote inhibition, as exemplified by the 3α-hydroxy-pregnane compounds, allopregnanolone and tetrahydro-deoxycorticosterone (THDOC), or conversely, inhibiting $GABA_A$ receptors, as is typical with sulphated neurosteroids such as pregnenolone sulphate and dehydroepiandrosterone sulphate. To date, most research has focussed on the former inhibition-enhancing steroids with less attention devoted to the mechanism of action of neurosteroids that instead inhibit $GABA_A$ receptors. Here, we address this deficit in our knowledge by studying in detail the modulation of inihibtory transmission onto hippocampal neurons produced by pregnenolone sulphate. Application of PS inhibited postsynaptic $GABA_A$ receptors expressed on principal hippocampal neurons in culture and in acute brain slices, as evident from decreases in IPSC amplitude and decay time. However, the more striking effect of PS is an increase in synaptic GABA release that appears to be mediated via a potentiation of presynaptic TRPM3 channels. Blockade of these presynaptic TRPM3 channels reveals another presynaptic target, inward rectifier potassium channels, by which PS causes a reduction in synaptic release of GABA.

PS effects on inhibitory synaptic transmission

Earlier studies showed that PS can modulate inhibitory synaptic transmission onto cultured hippocampal neurons (Teschemacher *et al.*, 1997; Mtchedlishvili & Kapur, 2003) and cerebellar Purkinje cells (Zamudio-Bulcock & Valenzuela, 2011). These reports highlighted divergent presynaptic actions of PS in decreasing and increasing GABA release onto postsynaptic hippocampal or cerebellar neurons respectively. The later cerebellar study also showed a postsynaptic inhibition of $GABA_A$ receptors by PS manifest as a decrease in mIPSC amplitude. This is consistent with the postsynaptic effects of PS in reducing IPSC amplitude and decay time that we report here and accords with studies showing inhibition of recombinant $GABA_A$ receptors by PS (Akk *et al.*, 2001; Seljeset *et al.*, 2018).

As noted above, a comparison of the impacts of PS on presynaptic GABA release reveals substantive differences between the various studies. Using a similar

concentration of PS as used in the current study (25 µM), Zamudio-Bulcock and Valenzuela (2011) demonstrate an increase in the frequency of mIPSCs recorded from cerebellar Purkinje cells (PCs) in acute brain slices from neonatal (P4 -10) rats. The two earlier hippocampal studies both investigated PS effects utilising cultured hippocampal neurons as we have here, although distinct concentration ranges of PS were employed: 0.1 – 50 µM (Teschemacher *et al.*, 1997); 300 pM – 1 µM (Mtchedlishvili & Kapur, 2003). Teschemacher *et al*., (1997) showed that higher concentrations of PS caused a reduction in sIPSC frequency. However, this effect had a slow time course and did not recover upon wash-out of PS, making it unlikely to be mediated by direct modulation of an ion channel. In contrast, Mtchedlishvili & Kapur (2003) found a significant reduction in IPSC frequency (both mIPSCs and sIPSCs) using concentrations of PS up to 1 µM and showed that this presynaptic effect of PS was mediated by pertussis toxin-sensitive σ1 receptors. It is unclear why there is a discrepancy between these earlier studies showing depression of synaptic GABA release and our results here demonstrating a striking enhancement of IPSC frequency with PS. One possibility is that with the higher concentrations of PS that we use here, σ1 receptors (or their downstream effectors) are either desensitised or internalised such that they no longer play a role in PS modulation of vesicular GABA release. Or it could simply be that expression levels of σ1 receptors in our cultured neurons are too low to support the role in reducing GABA release reported by Mtchedlishvili & Kapur (2003). Indeed, application of the selective σ1 receptor blocker BD-1063 had no impact upon the presynaptic effects of PS seen here (data not shown), which is consistent with either a lack of expression of σ1 receptors, or a limited functional role in presynaptic release in our cultures.

TRPM3 as a CNS target for PS

The TRPM3 receptor is a well-documented target of PS (Wagner *et al.*, 2008; Vriens *et al.*, 2011) and is expressed in various areas of human and rodent brain, including the choroid plexus, cerebellum and hippocampus (Oberwinkler *et al.*, 2005; Kunert-Keil *et al.*, 2006; Held & Toth, 2021). PS acts as an agonist at the TRPM3 receptor, increasing Ca^{2+} flux through the integral cation channel (Wagner *et al.*, 2008). However, little is known about the role of TRPM3 channels within the central nervous system, partly because to date, no structured analysis of expression across the brain has been performed, making it difficult to compare expression levels between

different brain areas and cell types. Expression of TRPM3 has been detected in neurons, epithelial cells and oligodendrocytes (Held & Toth, 2021) but of these, the functional impact of TRPM3 has only been confirmed in oligodendrocytes isolated from whole brain tissue (Hoffmann *et al.*, 2010) and in neurons from the developing cerebellum (Zamudio-Bulcock *et al.*, 2011). This latter study reported that TRPM3 is localised at glutamatergic synapses formed by climbing fibres onto Purkinje cells, providing a locus of action for PS to increase synaptic glutamate release (Zamudio-Bulcock *et al.*, 2011; Zamudio-Bulcock & Valenzuela, 2011). It was also apparent that TRPM3 is clustered at locations on PC somata distinct from glutamatergic synapses, with the authors speculating that these might represent GABAergic synapses (Zamudio-Bulcock *et al.*, 2011). This would correlate with the action of PS in potentiating synaptic GABA release onto neonatal rat PCs (Zamudio-Bulcock & Valenzuela, 2011).

Here, we provide evidence that TRPM3 channels are also expressed on hippocampal interneurons where their activation by PS results in an increase in synaptic GABA release onto postsynaptic pyramidal neurons. The enhancement in GABA release, evoked by PS, was apparent both in cultured hippocampal neurons and in CA1 pyramidal neurons in brain slices. Importantly, in both cases, the increase in release was blocked by the selective TRPM3 blocker ononetin. Notably, PS also increases GABA release in the presence of TTX, suggesting that transmission of action potentials is not required and that the PS targets must be located at, or close to, presynaptic GABA release sites. This is consistent with our immunocytochemistry showing partial colocalisation of TRPM3 clusters with both pre- and postsynaptic markers of inhibitory synapses. Hence, the presynaptic mechanism by which PS increases vesicular release of GABA likely involves increased Ca^{2+} influx via activation of TRPM3 channels located close to GABA release sites. This could either directly increase release by raising intracellular Ca^{2+} levels or could act indirectly via the depolarisation-induced activation of voltage-gated Ca^{2+} channels. Interestingly, PS has also been reported to increase glutamate release onto dentate gyrus hilar neurons via Ca^{2+}-induced Ca^{2+} release probably involving TRPM3 channels and intracellular ryanodine receptors (Lee *et al.*, 2010). This provides a further potential mechanism for the increase in GABA release that we observe here.

Kir 2.3 channels as a CNS target for PS

Unexpectedly, blockade of TRPM3 channels with ononetin, revealed an additional regulation of presynaptic GABA release by PS. This was of opposite polarity with 10 µM PS resulting in a greater than two-fold reduction in sIPSC frequency. Considering an earlier observation that PS at micromolar concentrations increases potassium currents mediated by Kir 2.3 channels (Kobayashi *et al.*, 2009), we performed further pharmacological dissection using the broad-spectrum K^+ channel blocker Ba^{2+} and the specific Kir2 channel antagonist ML133 (Wang *et al.*, 2011). Both Ba^{2+} and ML133 abolished the PS-evoked down-regulation in sIPSC frequency. Taken together with the earlier finding that PS selectively potentiates Kir2.3 channels compared with other inward rectifier potassium currents (Kir1.1, Kir2.1, Kir2.2 and Kir3.1/3.2, Kobayashi *et al*., 2009), this strongly implicates Kir2.3 channels as the presynaptic target involved in the PS-evoked depression of GABA release. Further support for this hypothesis is provided by our immunocytochemistry showing the expression of Kir2.3 at a subset of inhibitory synapses in cultured hippocampal neurons.

As far as we are aware, Kir2.3 channels have not been demonstrated to regulate neurotransmitter release. Kir2 channels are expressed in neurons throughout the brain, with Kir2.3 showing high levels of expression in the olfactory bulb, basal ganglia, cortex and cerebellar Purkinje cells and more moderate levels of expression in CA1 and CA2 hippocampus (Pruss *et al.*, 2005). Immuno-electron microscopy of the olfactory bulb has shown clustered expression of Kir2.3 at the postsynaptic membrane of excitatory synapses, suggesting a role for this channel in maintaining the membrane potential of spines and thereby regulating the activity of NMDA receptors in this compartment (Inanobe *et al.*, 2002). However, there appears to be no evidence to date detailing the regulation of inhibitory transmission by Kir2.3 and therefore, our results represent a new role for these inward-rectifying potassium channels.

PS as an endogenous modulator of brain function

The study of the neurophysiological roles of PS has been hampered due to difficulties in measuring low levels of this neurosteroid in rodent brain tissue (Schumacher *et al.*, 2008). Estimates of bulk concentrations of PS in rodent brain

tend to lie in the high picomolar to nanomolar range (Smith *et al.*, 2014). However, the presence of the enzymatic machinery required to synthesise PS within specific neuronal populations supports the idea of localised PS release that may drive vicinal concentrations significantly higher (Kimoto *et al.*, 2001; Smith *et al.*, 2014) with PS diffusion and cellular architecture likely to be influential. This idea is bolstered by a study showing that postsynaptic depolarisation of immature hippocampal neurons leads to the retrograde release of a PS-like molecule, resulting in an estimated synaptic concentration of 17 µM (Mameli *et al.*, 2005). Further evidence supporting local PS synthesis is provided by the observation that ethanol appears to increase synaptic levels of PS in hippocampal slices and that this increase is blocked by inhibition of a key biosynthetic pathway enzyme, P450scc, which converts cholesterol to pregnenolone (Mameli & Valenzuela, 2006). Hence, local concentrations of PS within the brain may indeed reach the micromolar levels that are demonstrated here to have significant impacts upon inhibitory transmission, both at postsynaptic sites, via inhibition of synaptic $GABA_A$ receptors, and at presynaptic GABA release sites, via activation of TRPM3 and Kir2.3 channels.

It is likely that the modulation of inhibitory synaptic transmission by endogenous PS within the brain will vary between different neuronal populations and at different developmental stages. If local PS levels are sufficiently high, we would predict relatively comparable effects postsynaptically, since PS generally shows little selectivity as a negative allosteric modulator between different $GABA_A$ receptor isoforms, with the exception of ρ1 homomeric receptors that are significantly less sensitive to inhibition by PS (Seljeset *et al.*, 2018). By contrast, we would expect presynaptic regulation of inhibitory synaptic transmission to vary significantly, even bidirectionally, depending upon the expression of various target effectors at presynaptic GABA release sites on interneurons. To date, three different presynaptic targets have been identified that can mediate PS modulation of synaptic GABA release: σ1 receptors (Mtchedlishvili & Kapur, 2003); TRPM3 receptors (Zamudio-Bulcock *et al.*, 2011) and this study; as well as Kir2.3 channels revealed also in this study. PS acts at TRPM3 channels to increase synaptic release, but decreases release via σ1 receptors and similarly by Kir2.3 channels. Therefore, the presynaptic modulation of GABAergic transmission by PS will be determined by the region-specific and developmental-dependent expression levels of these three targets on

interneurons within the CNS underpinning the diverse effects that PS can have on GABA release.

PS and synaptic plasticity at inhibitory synapses

It is very important for inhibitory synapses to be capable of dynamically responding to changing circumstances by regulating the release of GABA. The dominant presynaptic feature of the sulphated neurosteroid PS is an increase in IPSC frequency via TRPM3 activation. So, when will a decrease in release be evident under physiological conditions? This will depend on the activation status of TRPM3. It is clear that raised levels of phosphatidylinositol 4,5-bisphosphate (PIP2) or ATP can restore the activation status of TRPM3 from desensitization (Toth *et al.*, 2015). Thus, following the release of PS, conditions depleting PIP2 (including raised phosphatase activity or PLC activity, following GPCR activation, involving possibly m1AChR or Gq/11 linked receptors) may flip the presynaptic terminal from a high to a low probability of release, due to inhibition/desensitisation of TRPM3. Under these conditions, low probability release driven by PS activation of presynaptic Kir2.3 might predominate. Such a mechanism, although speculative, would provide a wide dynamic range for GABA release regulated by the triad of PS, TRPM3 and Kir2.3.

Finally, in regard to selectvity, PS is clearly a promiscous neurosteroid having effects on various targets, including specific voltage-gated sodium, calcium and potassium channels, TRPM3, σ1, AMPA/Kainate, NMDA and $GABA_A$ receptors (Smith *et al.*, 2014). Modulation of these various effectors allows PS to control presynaptic neurotransmitter release and postsynaptic neuronal excitability. Here, we elucidate the mechanisms by which PS controls inhibitory synaptic neurotransmission and identify the involvement of a novel target, Kir2.3 channels, in regulating synaptic GABA release. We predict that PS effects on inhibitory neurotransmission are likely to play a key role in the central neurophysiological actions of this endogenous neuromodulator.

References

Akk G, Bracamontes J & Steinbach JH. (2001). Pregnenolone sulfate block of GABA(A) receptors: mechanism and involvement of a residue in the M2 region of the alpha subunit. *J Physiol* **532,** 673-684.

Auger C, Kondo S & Marty A. (1998). Multivesicular release at single functional synaptic sites in cerebellar stellate and basket cells. *J Neurosci* **18,** 4532-4547.

Barberis A, Petrini EM & Cherubini E. (2004). Presynaptic source of quantal size variability at GABAergic synapses in rat hippocampal neurons in culture. *Eur J Neurosci* **20,** 1803-1810.

Belelli D & Lambert JJ. (2005). Neurosteroids: endogenous regulators of the GABAA receptor. *Nature Reviews Neuroscience* **6,** 565-575.

Flood JF, Farr SA, Johnson DA, Li PK & Morley JE. (1999). Peripheral steroid sulfatase inhibition potentiates improvement of memory retention for hippocampally administered dehydroepiandrosterone sulfate but not pregnenolone sulfate. *Psychoneuroendocrinology* **24,** 799-811.

Held K & Toth BI. (2021). TRPM3 in Brain (Patho)Physiology. *Front Cell Dev Biol* **9,** 635659.

Hoffmann A, Grimm C, Kraft R, Goldbaum O, Wrede A, Nolte C, Hanisch UK, Richter-Landsberg C, Bruck W, Kettenmann H & Harteneck C. (2010). TRPM3 is expressed in sphingosine-responsive myelinating oligodendrocytes. *J Neurochem* **114,** 654-665.

Inanobe A, Fujita A, Ito M, Tomoike H, Inageda K & Kurachi Y. (2002). Inward rectifier K+ channel Kir2.3 is localized at the postsynaptic membrane of excitatory synapses. *Am J Physiol Cell Physiol* **282,** C1396-1403.

Kimoto T, Tsurugizawa T, Ohta Y, Makino J, Tamura H, Hojo Y, Takata N & Kawato S. (2001). Neurosteroid synthesis by cytochrome p450-containing systems localized in the rat brain hippocampal neurons: N-methyl-D-aspartate and calcium-dependent synthesis. *Endocrinology* **142,** 3578-3589.

Kobayashi T, Washiyama K & Ikeda K. (2009). Pregnenolone sulfate potentiates the inwardly rectifying K channel Kir2.3. *PLoS One* **4,** e6311.

Kunert-Keil C, Bisping F, Kruger J & Brinkmeier H. (2006). Tissue-specific expression of TRP channel genes in the mouse and its variation in three different mouse strains. *BMC Genomics* **7,** 159.

Laverty D, Thomas P, Field M, Andersen OJ, Gold MG, Biggin PC, Gielen M & Smart TG. (2017). Crystal structures of a GABAA-receptor chimera reveal new endogenous neurosteroid-binding sites. *Nat Struct Mol Biol* **24,** 977-985.

Lee KH, Cho JH, Choi IS, Park HM, Lee MG, Choi BJ & Jang IS. (2010). Pregnenolone sulfate enhances spontaneous glutamate release by inducing presynaptic Ca2+-induced Ca2+ release. *Neuroscience* **171,** 106-116.

Mameli M, Carta M, Partridge LD & Valenzuela CF. (2005). Neurosteroid-induced plasticity of immature synapses via retrograde modulation of presynaptic NMDA receptors. *J Neurosci* **25,** 2285-2294.

Mameli M & Valenzuela CF. (2006). Alcohol increases efficacy of immature synapses in a neurosteroid-dependent manner. *Eur J Neurosci* **23,** 835-839.

Maninger N, Wolkowitz OM, Reus VI, Epel ES & Mellon SH. (2009). Neurobiological and neuropsychiatric effects of dehydroepiandrosterone (DHEA) and DHEA sulfate (DHEAS). *Front Neuroendocrinol* **30,** 65-91.

Mayo W, Dellu F, Robel P, Cherkaoui J, Le Moal M, Baulieu EE & Simon H. (1993). Infusion of neurosteroids into the nucleus basalis magnocellularis affects cognitive processes in the rat. *Brain Res* **607,** 324-328.

Miller PS, Scott S, Masiulis S, De Colibus L, Pardon E, Steyaert J & Aricescu AR. (2017). Structural basis for GABAA receptor potentiation by neurosteroids. *Nat Struct Mol Biol* **24,** 986-992.

Mtchedlishvili Z & Kapur J. (2003). A presynaptic action of the neurosteroid pregnenolone sulfate on GABAergic synaptic transmission. *Mol Pharmacol* **64,** 857-864.

Oberwinkler J, Lis A, Giehl KM, Flockerzi V & Philipp SE. (2005). Alternative splicing switches the divalent cation selectivity of TRPM3 channels. *J Biol Chem* **280,** 22540-22548.

Pruss H, Derst C, Lommel R & Veh RW. (2005). Differential distribution of individual subunits of strongly inwardly rectifying potassium channels (Kir2 family) in rat brain. *Brain Res Mol Brain Res* **139,** 63-79.

Schumacher M, Liere P, Akwa Y, Rajkowski K, Griffiths W, Bodin K, Sjovall J & Baulieu EE. (2008). Pregnenolone sulfate in the brain: a controversial neurosteroid. *Neurochem Int* **52,** 522-540.

Seljeset S, Bright DP, Thomas P & Smart TG. (2018). Probing GABAA receptors with inhibitory neurosteroids. *Neuropharmacology* **136,** 23-36.

Seljeset S, Laverty D & Smart TG. (2015). Inhibitory neurosteroids and the GABAA receptor. *Adv Pharmacol* **72,** 165-187.

Smart TG & Paoletti P. (2012). Synaptic Neurotransmitter-Gated Receptors. *Cold Spring Harbor Perspectives in Biology* **4,** a009662-a009662.

Smith CC, Gibbs TT & Farb DH. (2014). Pregnenolone sulfate as a modulator of synaptic plasticity. *Psychopharmacology (Berl)* **231,** 3537-3556.

Teschemacher A, Kasparov S, Kravitz EA & Rahamimoff R. (1997). Presynaptic action of the neurosteroid pregnenolone sulfate on inhibitory transmitter release in cultured hippocampal neurons. *Brain Res* **772,** 226-232.

Toth BI, Konrad M, Ghosh D, Mohr F, Halaszovich CR, Leitner MG, Vriens J, Oberwinkler J & Voets T. (2015). Regulation of the transient receptor potential channel TRPM3 by phosphoinositides. *J Gen Physiol* **146,** 51-63.

Vankova M, Hill M, Velikova M, Vcelak J, Vacinova G, Dvorakova K, Lukasova P, Vejrazkova D, Rusina R, Holmerova I, Jarolimova E, Vankova H, Kancheva R, Bendlova B & Starka L. (2016). Preliminary evidence of altered steroidogenesis in women with Alzheimer's disease: Have the patients "OLDER" adrenal zona reticularis? *J Steroid Biochem Mol Biol* **158,** 157-177.

Vriens J, Owsianik G, Hofmann T, Philipp SE, Stab J, Chen X, Benoit M, Xue F, Janssens A, Kerselaers S, Oberwinkler J, Vennekens R, Gudermann T, Nilius B & Voets T. (2011). TRPM3 is a nociceptor channel involved in the detection of noxious heat. *Neuron* **70,** 482-494.

Wagner TF, Loch S, Lambert S, Straub I, Mannebach S, Mathar I, Dufer M, Lis A, Flockerzi V, Philipp SE & Oberwinkler J. (2008). Transient receptor potential M3 channels are ionotropic steroid receptors in pancreatic beta cells. *Nat Cell Biol* **10,** 1421-1430.

Wang HR, Wu M, Yu H, Long S, Stevens A, Engers DW, Sackin H, Daniels JS, Dawson ES, Hopkins CR, Lindsley CW, Li M & McManus OB. (2011). Selective inhibition of the K(ir)2 family of inward rectifier potassium channels by a small

molecule probe: the discovery, SAR, and pharmacological characterization of ML133. *ACS Chem Biol* **6,** 845-856.

Weill-Engerer S, David JP, Sazdovitch V, Liere P, Eychenne B, Pianos A, Schumacher M, Delacourte A, Baulieu EE & Akwa Y. (2002). Neurosteroid quantification in human brain regions: comparison between Alzheimer's and nondemented patients. *J Clin Endocrinol Metab* **87,** 5138-5143.

Wong P, Sze Y, Chang CC, Lee J & Zhang X. (2015). Pregnenolone sulfate normalizes schizophrenia-like behaviors in dopamine transporter knockout mice through the AKT/GSK3beta pathway. *Transl Psychiatry* **5,** e528.

Zamudio-Bulcock PA, Everett J, Harteneck C & Valenzuela CF. (2011). Activation of steroid-sensitive TRPM3 channels potentiates glutamatergic transmission at cerebellar Purkinje neurons from developing rats. *J Neurochem* **119,** 474-485.

Zamudio-Bulcock PA & Valenzuela CF. (2011). Pregnenolone sulfate increases glutamate release at neonatal climbing fiber-to-Purkinje cell synapses. *Neuroscience* **175,** 24-36.

Additional Information

Data availability statement

All the data that constitutes our results are included in the manuscript and associated figures.

Competing interests

There are no competing interests

Author contributions

Sandra Seljeset: Conceptualization, Formal analysis, Methodology, Investigation, Writing - original draft, Writing - review & editing; **Seth Liebowitz**: Investigation; **Damian Bright**: Conceptualization, Formal analysis, Methodology, Investigation, Supervision, Writing - original draft, Writing - review & editing; **Trevor Smart**: Conceptualization, Formal analysis, Methodology, Supervision, Writing - review & editing, Funding acquisition.

Funding

SS was supported by a Wellcome Trust PhD studentship. The study was supported by an MRC programme grant (MR/K005537/1).

Figure legends

Figure 1. PS increases sIPSC frequency in hippocampal neurons

A, representative membrane currents recorded from cultured hippocampal neurons showing sIPSCs under control conditions and in the presence of the indicated PS concentrations. **B**, summary plot showing the effect of various PS concentrations on normalised sIPSC frequency relative to control. In this, and subsequent plots, circles represent individual cells, whilst bars with errors represent the mean ± SEM and dashed lines indicate the normalised control value (either unity or 100 %). ** $p < 0.01$, **** $p < 0.0001$, assessed by two-way RM ANOVA, followed by Sidak's multiple comparisons tests with respect to control. **C**, time-course plot of 3 µM PS on sIPSC frequency. Symbols with error bars indicate the mean ± SEM sIPSC frequency recorded in control (black), in the presence of 3 µM PS (magenta) and after wash-out of PS (green).

Figure 2. Postsynaptic effects of PS

A, mean sIPSC waveforms recorded from a representative hippocampal neuron in control conditions (black) and in the presence of 3 µM PS (magenta). Inset shows the same mean sIPSC waveforms but scaled to the same peak amplitude to highlight the effect of PS accelerating the sIPSC decay. **B**, summary plot showing the effect of various PS concentrations on normalised sIPSC amplitude relative to control. **C**, summary plot showing the effects of 1 and 3 µM PS on normalised sIPSC decay relative to control. * $p < 0.05$, ** $p < 0.01$, *** $p < 0.001$, assessed by two-way ANOVA, followed by Sidak's multiple comparisons tests with respect to control. **D-G**, analysis of sIPSC amplitudes for synaptic events recorded from neurons exposed either to 3 µM PS (control **D**; **+** PS **E**, plots include 200 events taken from each of 8 neurons, 1600 total events per condition) or to 10 µM PS (control **F**; + PS **G**, 200 events taken from each of 7 neurons, 1400 total per condition). Amplitude distributions are fitted with the sum of two Gaussians (**D**, **E**, **F**, individual Gaussians in magenta, sum in blue) or with a single Gaussian (**G**, blue).

Figure 3. Effects of PS on mIPSCs

A, representative membrane currents recorded from cultured hippocampal neurons showing control mIPSCs in 500 nM TTX and following the addition of 1-10 µM PS. **B**,

summary plot showing the effects of 1, 3 and 10 µM PS on normalised mIPSC frequency relative to TTX alone. **C**, summary plot showing the normalised mIPSC amplitude in the presence of 1, 3 and 10 µM PS relative to TTX alone. **D**, peak-scaled mean mIPSC waveforms recorded from a representative hippocampal neuron in TTX alone (black) and in the presence of 3 µM PS (magenta). **E**, summary plot showing the effects of 1, 3 and 10 µM PS on normalised mIPSC decay relative to TTX alone. * $p < 0.05$, ** $p < 0.01$, **** $p < 0.0001$, assessed by two-way ANOVA, followed by Sidak's multiple comparisons tests with respect to TTX alone. **F-H**, analysis of mIPSC amplitudes for synaptic events recorded from neurons exposed to 1 µM PS (**F,** plots include 100 events taken from each of 7 neurons, 700 total events per condition), 3 µM PS (**G,** plots include 200 events taken from each of 8 neurons, 1600 total events per condition) or 10 µM PS (**H,** plots include 100 events taken from each of 6 neurons, 600 total events per condition). Amplitude distributions are fitted with the sum of two Gaussians with the individual Gaussians in magenta and the sum in blue.

Figure 4. PS increases synaptic GABA release via TRPM3 channels

A, Membrane currents recorded from a cultured hippocampal neuron showing sIPSCs under control conditions and after sequential application of ononetin followed by PS (both 10 µM). **B**, **C**, summary plots showing the effects of ononetin alone, and PS with ononetin, on normalised sIPSC frequency (**B**) and amplitude (**C**) both relative to control. ** $p < 0.01$, *** $p < 0.001$ with respect to control, ## $p < 0.01$ with respect to ononetin alone, assessed by one-way ANOVA, followed by Tukey's multiple comparisons tests. **D**, a sample of mIPSCs recorded in the presence of TTX (500 nM) and ononetin (10 µM) before co-application of PS (10 µM). **E**, **F**, summary plots showing the effects of PS on normalised mIPSC frequency (**E**) and amplitude (**F**) both relative to ononetin alone. * $p < 0.05$, ** $p < 0.01$. **G**, confocal images of hippocampal dendrites showing immunoreactivity for TRPM3 (green) and MAP2 (magenta). The lower image illustrates the effect of performing immunostaining after pre-adsorption of the TRPM3 antibody with a negative control antigen. **H**, **I**, confocal images of hippocampal dendrites showing immunoreactivity for TRPM3 (green) and

GAD65 (magenta, **H**) or gephyrin (magenta, **I**). Arrowheads indicate regions of colocalization. Scale bars in **G, H** and **I** = 10 µm.

Figure 5. PS decreases synaptic GABA release via Kir2.3 channels

A, membrane currents recorded from a cultured hippocampal neuron showing sIPSCs in control conditions and after sequential application of Ba^{2+} (3 mM), followed by ononetin and PS (both 10 µM). **B**, summary plot showing the effects of Ba^{2+}, and PS in the presence of Ba^{2+} and ononetin on normalised sIPSC frequency relative to control. ** $p < 0.01$, *** $p < 0.001$, with respect to control, ns = non-significant with respect to Ba^{2+} alone, assessed by one-way RM ANOVA, followed by Tukey's multiple comparisons tests. **C**, membrane currents recorded from a hippocampal neuron showing sIPSCs in ononetin (10 µM) and after sequential application of ML133 (100 µM) and PS (10 µM). **D**, summary plot showing the effects of ML133 (ML) in the presence of ononetin (On), and after co-application of PS, on normalised sIPSC frequency relative to ononetin alone. *** $p < 0.001$, with respect to ononetin alone, ns = non-significant with respect to ononetin and ML133, assessed by one-way RM ANOVA, followed by Tukey's multiple comparisons tests. **E**, **F**, confocal images of hippocampal dendrites showing immunoreactivity for Kir2.3 (green) and GAD65 (magenta, **E**) or gephyrin (magenta, **F**). Arrowheads indicate regions of colocalization. **G**, confocal images of hippocampal dendrites showing immunoreactivity for Kir2.3 (green) and MAP2 (magenta). The lower image illustrates the effect of performing immunostaining after pre-adsorption of the Kir2.3 antibody with a negative control antigen. Scale bars in **E** (for **F** also) and **G** = 10 and 5 µm, respectively.

Figure 6. PS increases synaptic GABA release onto CA1 pyramidal cells via TRPM3 channels

A, representative membrane currents recorded from a hippocampal CA1 pyramidal cell (PC) in an acute brain slice showing sIPSCs in control conditions and in the presence of 10 µM PS. The inset shows representative mean sIPSC waveforms recorded in control conditions (black) and after the application of 10 µM PS (magenta). **B**, summary plots showing the effects of 10 µM PS on normalised sIPSC frequency and decay relative to control. * $p < 0.05$ with respect to control, assessed by paired t test. **C**, membrane currents recorded from a CA1 PC showing sIPSCs in

control conditions and after the sequential application of ononetin followed by PS (both 10 µM). **D**, summary plot showing the normalised sIPSC frequency in the presence of ononetin alone and in ononetin plus PS. * $p < 0.05$, ** $p < 0.01$, with respect to control, ns = non-significant with respect to ononetin alone, assessed by one-way RM ANOVA, followed by Tukey's multiple comparisons tests.

		Mean IPSC frequency (Hz)	Mean IPSC amplitude (-pA)
PS effects on sIPSCs (Figures 1 & 2)	Control (n = 6) 30 nM PS	0.5 ± 0.5 1.0 ± 1.4	82.1 ± 42.6 70.0 ± 38.1
	Control (n = 6) 1 µM PS	2.6 ± 1.5 5.6 ± 4.3	106.0 ± 24.2 60.2 ± 24.7
	Control (n = 11) 3 µM PS	1.7 ± 2.0 8.0 ± 8.4	64.6 ± 28.3 40.8 ± 14.1
	Control (n = 12) 10 µM PS	2.6 ± 1.3 12.5 ± 7.3	64.0 ± 29.3 40.7 ± 22.4
PS effects on mIPSCs (Figure 3)	Control (n = 8) 1 µM PS	1.7 ± 0.6 1.7 ± 0.8	47.8 ± 7.2 45.8 ± 8.8
	Control (n = 8) 3 µM PS	1.7 ± 0.2 4.6 ± 1.0	41.8 ± 3.2 36.5 ± 1.9
	Control (n = 6) 10 µM PS	1.0 ± 0.6 9.7 ± 1.9	36.5 ± 6.5 32.7 ± 2.5
Ononetin + PS on sIPSCs (Figure 4)	Control (n = 11) Ononetin Ononetin + PS	2.6 ± 0.8 1.9 ± 0.6 0.7 ± 0.2	76.1 ± 7.4 76.5 ± 7.7 47.5 ± 4.5
Ononetin + PS on mIPSCs (Figure 4)	Ononetin (n = 7) Ononetin + PS	2.0 ± 0.6 1.1 ± 0.2	47.3 ± 6.5 31.4 ± 3.8
PS effects on sIPSCs in Ba^{2+} (Figure 5)	Control (n = 6) Ba^{2+} Ba^{2+} + Ononetin + PS	1.3 ± 0.4 14.0 ± 3.8 18.3 ± 4.2	175.5 ± 27.8 100.5 ± 9.9 53.4 ± 5.7
PS effects on sIPSCs in ML133 (Figure 5)	Ononetin (n = 8) Ononetin + ML133 Ononetin + ML133 + PS	1.0 ± 0.4 10.1 ± 2.2 9.2 ± 2.0	77.1 ± 19.1 46.1 ± 5.0 38.7 ± 4.1
PS effects on sIPSCs in CA1 PCs (Figure 6)	Control (n = 6) PS	1.0 ± 0.5 1.5 ± 0.4	18.3 ± 2.4 17.3 ± 1.4
Ononetin + PS on sIPSCs in CA1 PCs (Figure 6)	Control (n = 6) Ononetin Ononetin + PS	0.4 ± 0.1 0.8 ± 0.2 0.9 ± 0.2	20.7 ± 3.2 20.7 ± 1.6 19.0 ± 1.6

Table 1. IPSC frequencies and amplitudes

Table shows mean (± SEM) IPSC frequencies and amplitudes for all recordings in cultured hippocampal neurons (Figures 1-5) and in CA1 pyramidal in acute rat brain slices (Figure 6). Concentrations of drugs, unless stated otherwise, are 10 µM PS, 10 µM ononetin, 3 mM Ba^{2+} and 100 µM ML133. mIPSCs were recorded in 500 nM TTX.

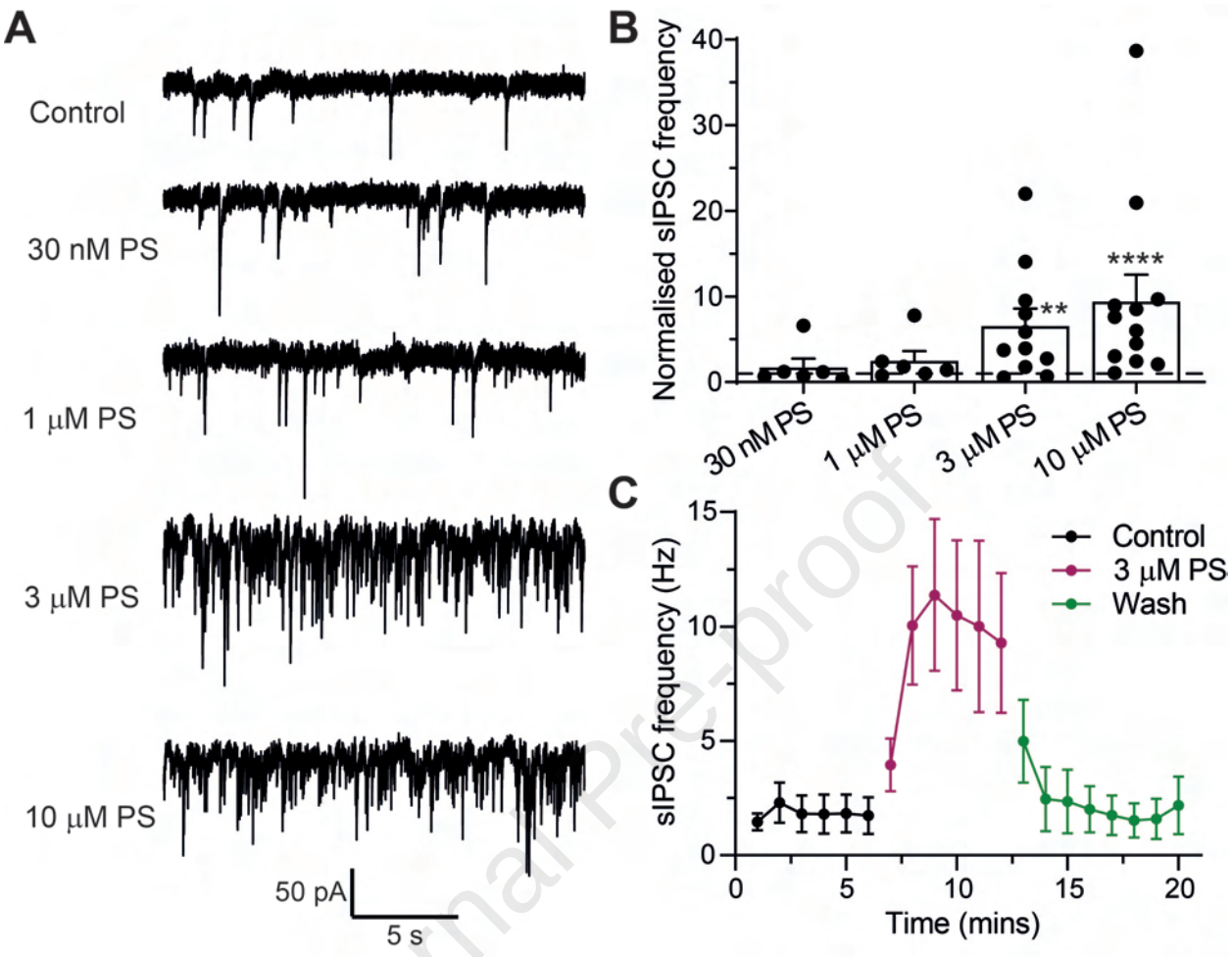

Figure 1

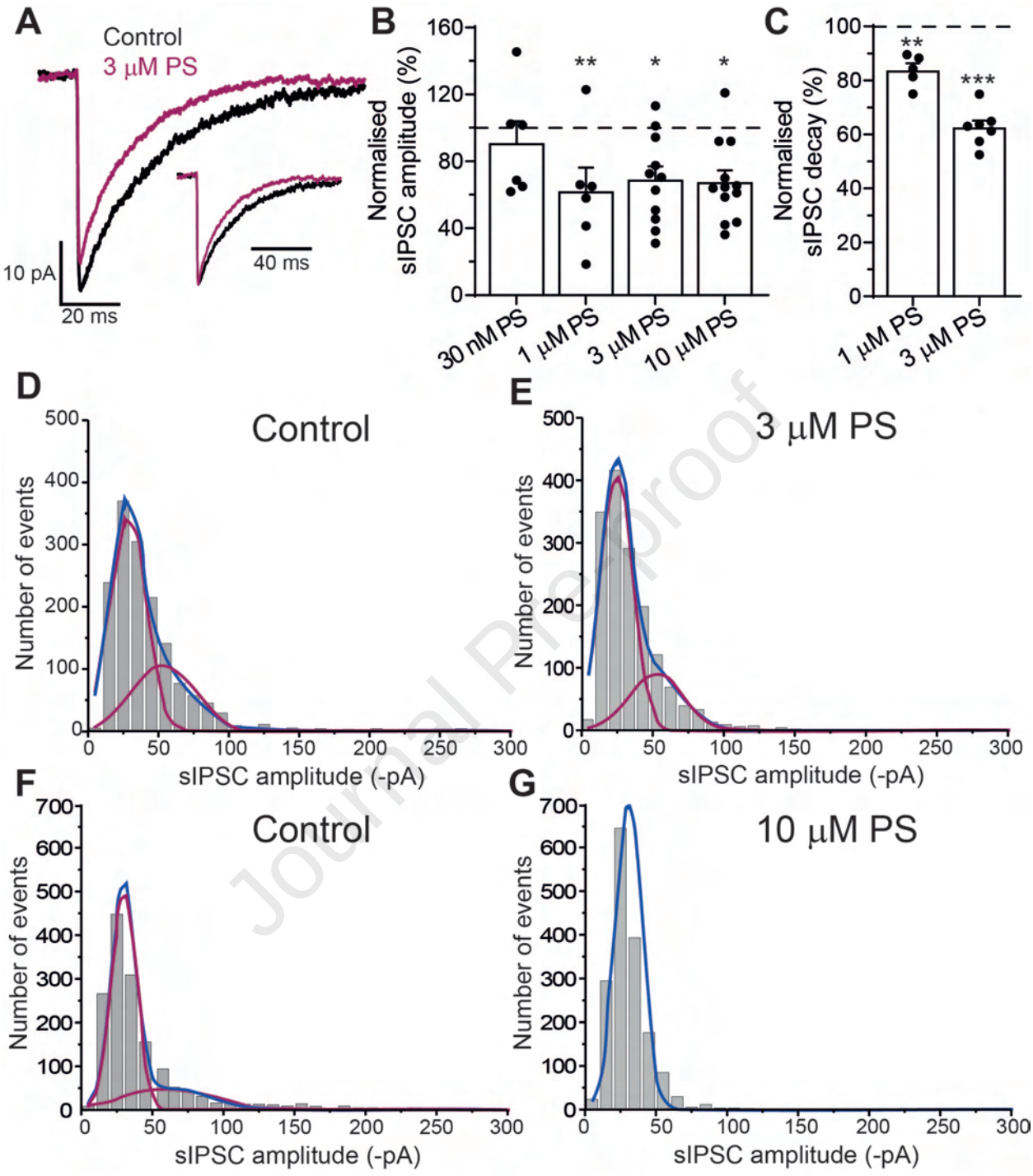
A
Control
3 μM PS
10 pA
20 ms
40 ms
B
Normalised sIPSC amplitude (%)
30 nM PS
1 μM PS
3 μM PS
10 μM PS
C
Normalised sIPSC decay (%)
1 μM PS
3 μM PS
D
Control
E
3 μM PS
F
Control
G
10 μM PS
Number of events
sIPSC amplitude (-pA)

Figure 2

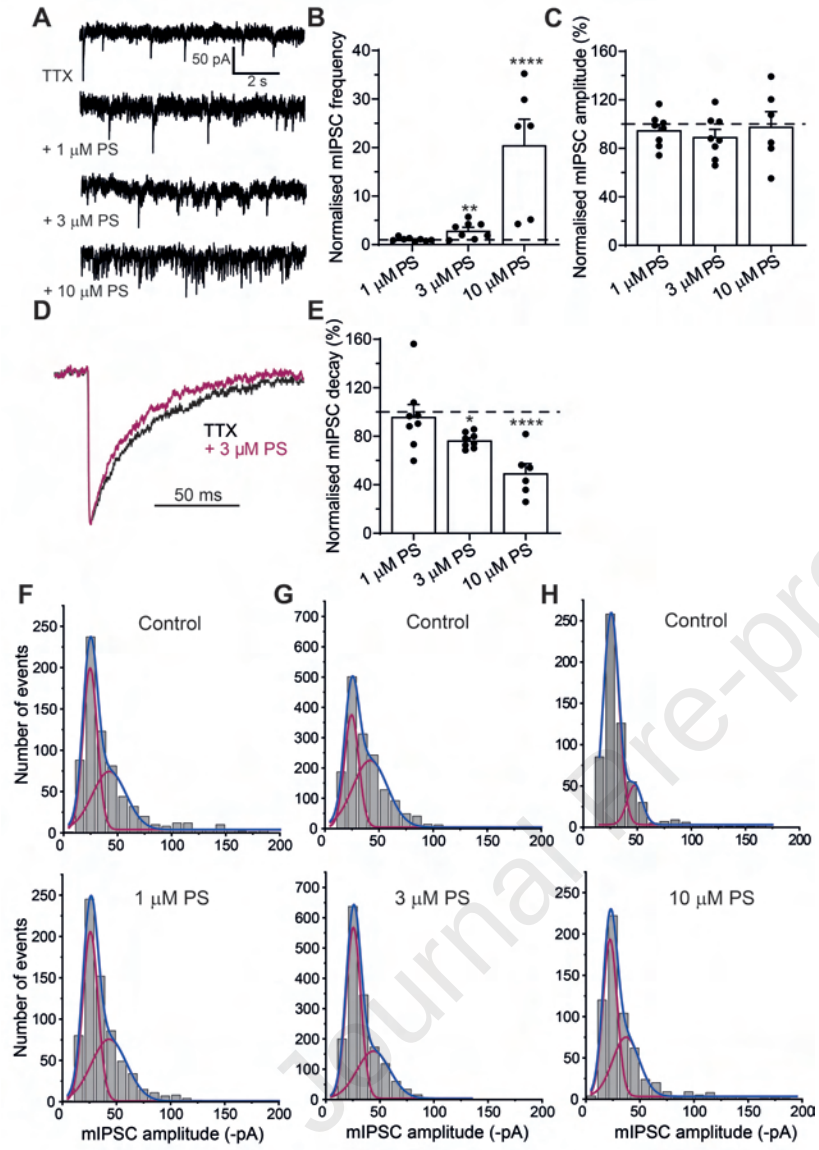

Figure 3

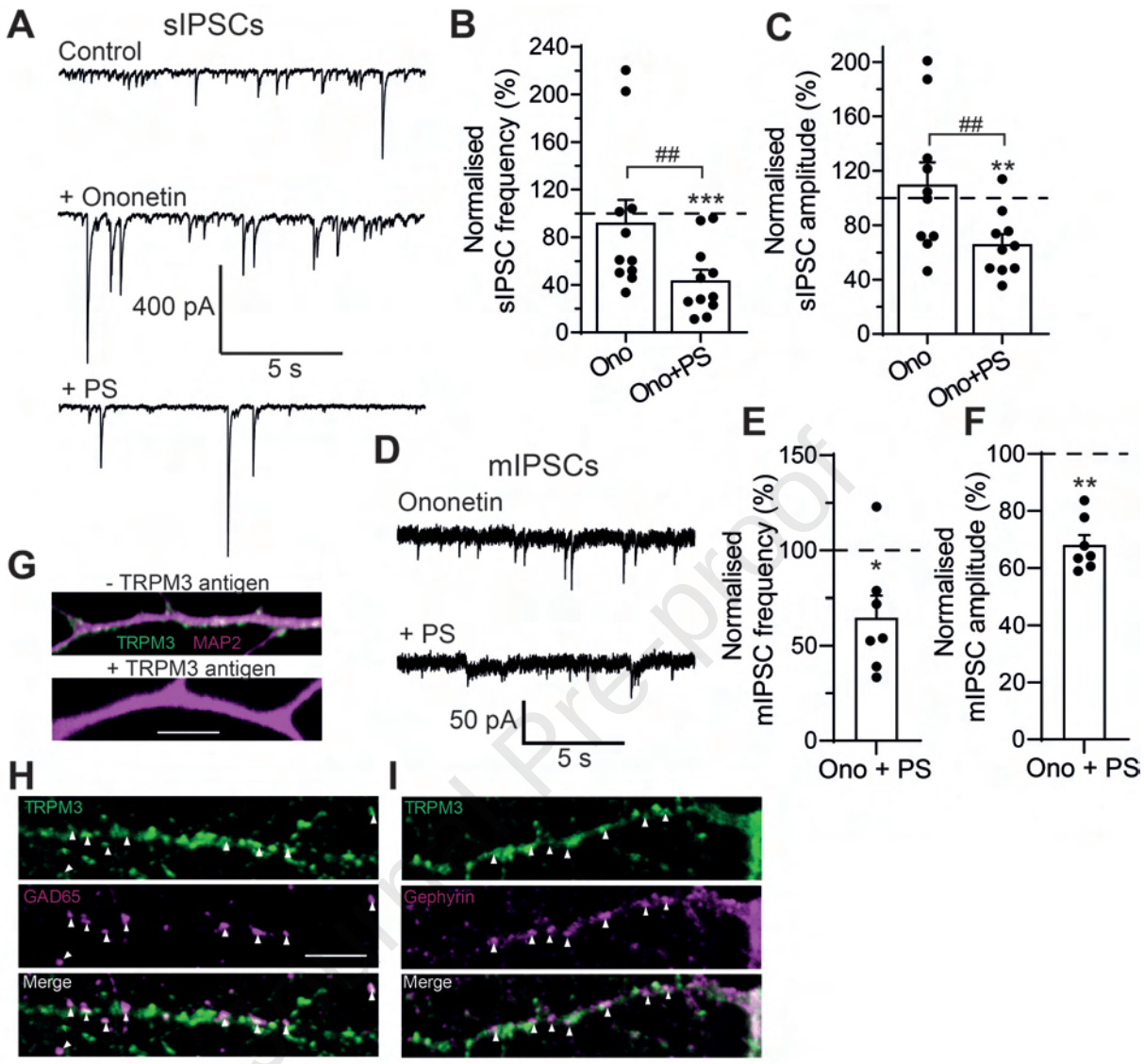
A
sIPSCs
Control
+ Ononetin
400 pA
5 s
+ PS
B
Normalised sIPSC frequency (%)
240
200
160
120
80
40
0
##
***
Ono
Ono+PS
C
Normalised sIPSC amplitude (%)
200
160
120
80
40
0
##
**
Ono
Ono+PS
D
mIPSCs
Ononetin
+ PS
50 pA
5 s
E
Normalised mIPSC frequency (%)
150
100
50
0
*
Ono + PS
F
Normalised mIPSC amplitude (%)
100
80
60
40
20
0
**
Ono + PS
G
- TRPM3 antigen
TRPM3
MAP2
+ TRPM3 antigen
H
TRPM3
GAD65
Merge
I
TRPM3
Gephyrin
Merge

Figure 4

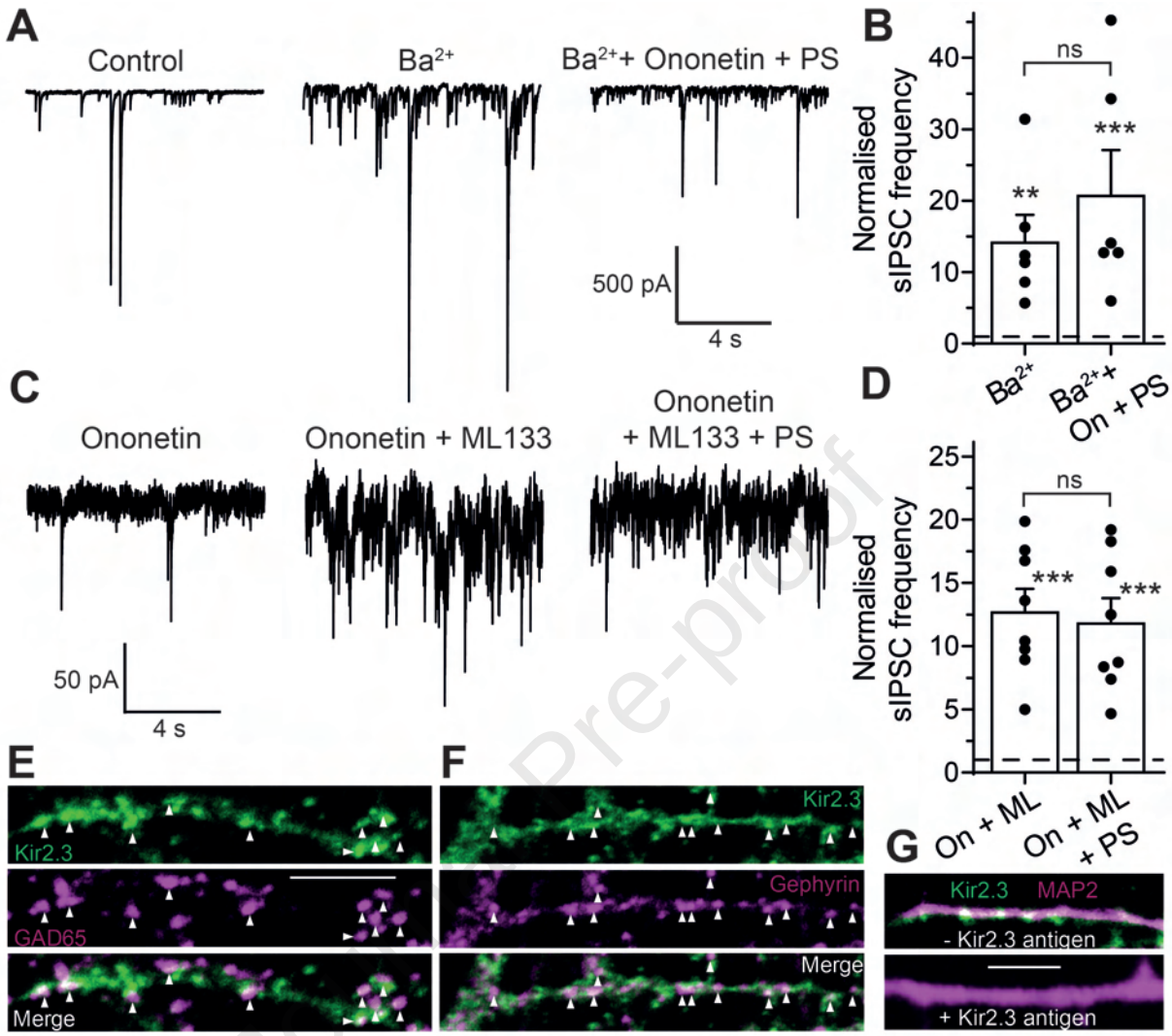

Figure 5

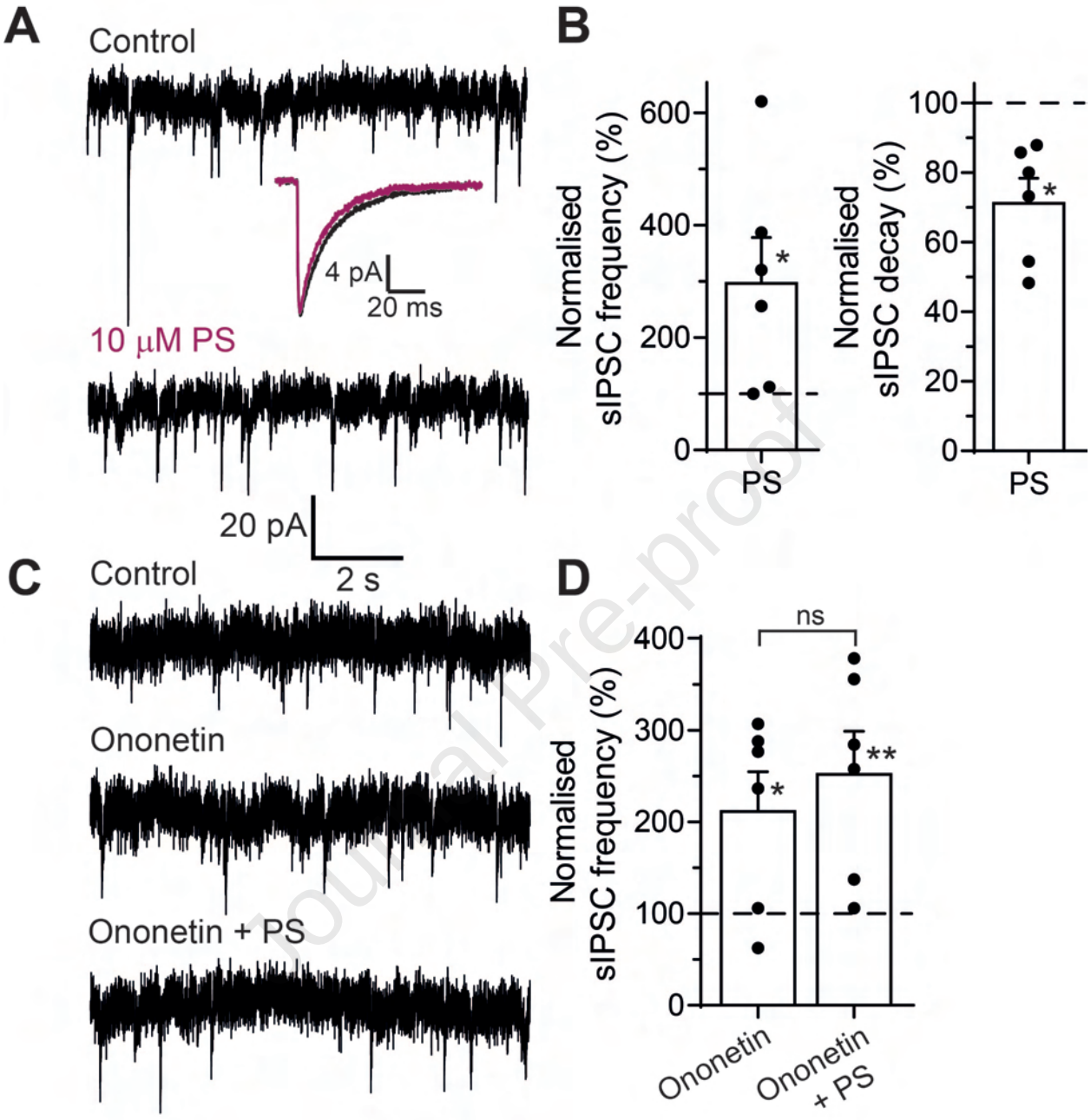

Figure 6

Highlights

- Pregnenolone sulphate (PS) is an endogenous brain neurosteroid
- PS modulates hippocampal inhibitory synaptic transmission
- PS blocks postsynaptic $GABA_A$ receptors to decrease IPSC amplitude and decay time
- PS activates presynaptic TRPM3 channels to increase synaptic GABA release
- Block of TRPM3 reveals a PS-evoked reduction in GABA release via Kir2 channels

Competing interests

There are no competing interests